Middle-ultraviolet laser photoelectron emission from vertically aligned millimeter-long multiwalled carbon nanotubes

Parham Yaghoobi, Mario Michan, and Alireza Nojeh[a)]
Department of Electrical and Computer Engineering, The University of British Columbia, Vancouver, British Columbia V6T 1Z4, Canada

(Received 7 August 2010; accepted 14 September 2010; published online 13 October 2010)

We demonstrate photoelectron emission from millimeter-long forests of vertically aligned multiwalled carbon nanotubes using 266 nm light, which illuminates the forests from the side. We have measured quantum efficiencies in the order of $\sim 10^{-5}$ at low fields (pure photoemission) and $\sim 10^{-3}$ at an applied field of 0.3 V μm^{-1}, which are 2–4 orders of magnitude higher than those obtained from films of randomly oriented nanotubes, and approach the quantum efficiency of semimetal photocathodes. Through optical simulations we show that 266 nm light is absorbed within the first few layers of the nanotube forest. © *2010 American Institute of Physics*. [doi:10.1063/1.3496486]

Interaction of light with carbon nanotubes (CNTs) has been an area of interest in recent years, for example, it has been predicted that photonic crystals can be made for visible and deep ultraviolet (UV) light from CNT forests by tuning the internanotube spacing,[1] and an electron beam can stimulate electromagnetic radiation from a single-walled carbon nanotube (SWNT).[2] Photoemission, a process by which an electron is emitted from a material into vacuum by absorbing energy from photons, has applications in accelerators (e.g., rf photocathode for free electron lasers)[3] to ultrahigh-speed (gigahertz) electron sources for microwave vacuum electronics.[4] The main focus of previous research in photoemission from CNTs has been on photoemission spectroscopy, typically performed with photon energies of greater than 10 eV, which is much higher than the work function of CNTs (~4–5 eV), for studying electronic structure and the binding energies.[5,6]

The study of photoemission from CNTs with photon energies of a few electron volts for device applications (i.e., photocathodes) has been limited. We previously demonstrated photoemission using a 266 nm (4.66 eV) laser from sparse collections of SWNTs lying on a substrate.[7] It appeared that the absorption cross-section of a SWNT is larger than its geometrical cross-section, suggesting efficient absorption mechanisms based on optical antenna effects. Wong *et al.*[8] used pulsed lasers (at 532, 355, and 266 nm) to observe photoemission from a matt of horizontal, randomly distributed multiwalled carbon nanotubes (MWNTs) on a surface, with lengths in the 5–10 μm range. They concluded that at 532 and 355 nm the electron emission mechanism was purely thermal; at 266 nm they observed photoemission with a quantum efficiency of $\sim 10^{-7}$ under an applied electric field of 1.67 V μm^{-1}, which is in the same order of magnitude as fields needed for field-emission from CNTs.[9] Hudanski *et al.*[10] demonstrated a photocathode that uses silicon photodiodes to control electron emission from MWNT field-emitters. Westover *et al.* have demonstrated photo- and thermionic emisson from potassium-intercalated carbon nanotube arrays.[11]

The highest quantum efficiencies for photocathodes (>10%) are obtained from a mixture of multilayer semimetals and alkali metals, in particular cesium. However, these materials are highly sensitive and have to be made and operated in ultrahigh vacuum (better than 10^{-10} Torr) and have a short operating life time. Metal photocathodes, on the other hand, are more robust and can be operated at lower vacuum conditions ($\sim 10^{-6}$ Torr); however, they have much lower quantum efficiencies, for example, a copper photocathode has a quantum efficiency of $\sim 10^{-5}$ for 266 nm light.[12]

In this work, we demonstrate photoemission from vertically aligned, millimeter-long forests of MWNTs with a quantum efficiency of $\sim 10^{-5}$ at an applied electric field of only ~1 V mm^{-1} (only used for the collection of electrons by the anode), which is purely photoemission, and a quantum efficiency of $\sim 10^{-3}$ at an applied field of 0.3 V μm^{-1}. Our simulations demonstrate that the absorption happens within the first few tens of nanometers of the forest when light is incident from the side.

Milimeter-long, aligned forests of MWNTs were grown on a highly p-doped Si wafer using atmospheric-pressure chemical vapor deposition. As catalyst, 1 nm of iron was evaporated on 10 nm of alumina on the Si wafer prior to nanotube growth. For each growth, the sample was heated up to 750 °C under a flow of 400 SCCM of Ar. The flow was maintained at 750 °C for 15 min before the sample was annealed for 3 min under 500 SCCM of H_2 and 200 SCCM of Ar. Immediately after annealing, a flow of 140 SCCM of C_2H_4 was introduced for an hour to grow the CNT forests. The sample was then cooled down under a flow of 400 SCCM of Ar. As can be seen from the scanning electron micrograph of the side of the forest (Fig. 1 inset), the CNTs are overall aligned in the vertical direction.

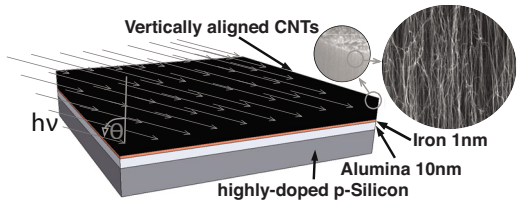

FIG. 1. (Color online) CNT forests were grown on 1 nm of iron and 10 nm of alumina. The laser illuminated the forest at an angle θ with respect to the axis of the CNTs. The scanning electron micrograph close-up of the side of the forest (inset) shows the overall aligned nature of CNTs in the forest.

a)Electronic mail: anojeh@ece.ubc.ca.

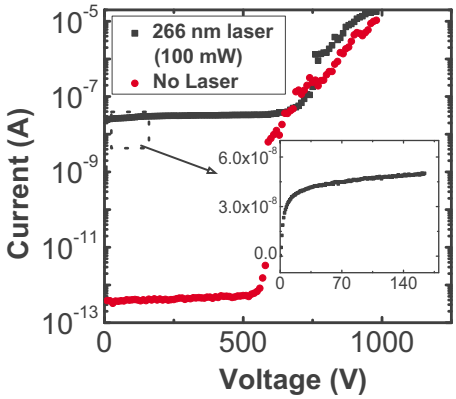

FIG. 2. (Color online) Photoemission I-V characteristics of the CNT forest with and without the 266 nm laser (incident at 90° to the CNTs) with a typical anode spacing of ~3 mm from the top surface of the CNT forest (error bars are smaller than the graph markers and are masked by them). Inset: nonlogarithmic plot of the first 150 V.

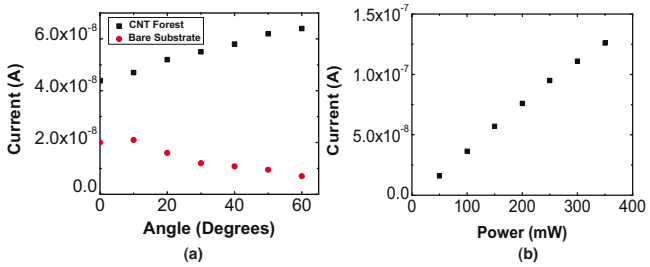

FIG. 3. (Color online) (a) Emission current vs angle of rotation (θ) for the CNT forest and the control device (catalyst on substrate but no CNT). (b) Emission current from CNT forest vs the 266 nm laser power under a 100 V bias voltage.

The nanotube sample was then placed in a custom-made holder, where it served as the cathode. A metallic wire, placed at a distance of ~3 mm from the top surface of the CNT forest, served as the anode/collector. The sample holder was placed on a rotating arm in a high-vacuum chamber pumped down to $\sim 10^{-8}$ Torr using a dry (turbomolecular) pump. A 532 nm laser (Coherent Verdi V-5) was then used to generate a 266 nm UV beam using a frequency doubler (Spectra-Physics Wavetrain), which was guided into the vacuum chamber through a sapphire viewport (UV transparency of 70%) and onto the CNT forest (Fig. 1). To apply a collection voltage and measure the collected current at the anode, a Keithley 6517A source/electrometer was used.

Figure 2 illustrates the I-V characteristics of the CNT forest both with 100 mW of continuous-wave 266 nm laser (incident at an angle of θ=90°, i.e., illuminating the side of the forest) and without laser. The photoemission current quickly ramps up to its maximum at a collection field of ~0.33 V mm^{-1} (Fig. 2 inset), which is far below the threshold of field emission. Up to a voltage of ~600 V (collection field of 0.2 V μm^{-1}), no field-emission is observed and an almost constant photoemission current of ~30 nA is obtained. At higher voltages, we start to see field-emission from the forest and even without light there is significant current. The current measurement error is about 10^{-13} A.

To confirm that (at least the majority of) photoemission is occurring from the CNTs and not the substrate, two experiments were carried out. First, we did a stopping voltage test, where we applied a negative bias to the anode until no current was measured through it. Second, we performed a rotation test, in which we changed the angle of incidence of light. Both tests were carried out on two samples, one including a CNT forest and another with only the Si substrate and the catalyst (alumina/iron).

In principle, the stopping voltage test can also reveal the work function of the emitting material, since the stopping voltage corresponds to the kinetic energy of the emitted electrons, which is the difference between the incident photon energy and work function. However, this is a rather simplistic view based on neglecting the energy distribution of the electrons, the emission of phonons and effects such as two-photon absorption. In addition, it assumes no contact resistance at the cathode and anode. Therefore, in practice we were not able to measure the work function on an absolute scale. However, this test is still useful since the difference between the two samples is only the CNT forest and if the measured stopping voltage is different in the two cases, then one may conclude that the emitted electrons are originating from materials with different work functions. Indeed, the measured stopping voltages were considerably different: for the sample with CNT forest, we measured a stopping voltage of ~0.02 eV, whereas for the sample with catalyst only, we measured ~0.2 eV. This method was also used to ensure that the emitted electrons from the CNTs are due to photoemission and not a thermionic process (laser heating of the CNTs). The intensity of the laser was increased while the anode was biased at the stopping voltage and no increase in emitted current was measured. Had thermionic emission been the case, electrons with higher kinetic energies would have been emitted at higher laser intensities (higher temperatures), overcoming the stopping-voltage barrier.

In the rotation test, we gradually changed the direction of different devices with respect to the angle of incidence of the laser beam, while keeping the applied voltage and the distance between the anode and cathode constant (the anode also rotated with the sample) in order to keep the collection field constant. The results are shown in Fig. 3(a). The photoemission current decreases as we rotate the sample with only Si wafer and catalyst, as opposed to the behavior of the device containing the CNT forest (this was tested on two different nanotube forests). This difference in behavior is yet another indication that the electrons are being emitted from different materials in the two cases (in one case from the substrate/catalyst and in the other from the nanotubes).

The increase in photoemission current as the angle θ is increased may be explained as follows: for small θ, the laser illuminates the forest mainly from the top, i.e., light only hits the tips of the nanotubes. Given the sparse nature of the forests (our characterization reveals that they are more than 85% empty space), only a small portion of the light is expected to be absorbed by the nanotubes. Moreover, in this case the electric field of light is mostly in the direction perpendicular to the nanotube axis. As the angle θ is increased and the forest is illuminated more from the side, the effective area covered by nanotubes in the beam path grows larger. In addition, the component of the laser's electric field along the tube axis grows with θ, favoring stronger emission. In the case of the sample with only catalyst (11 nm in thickness), increasing θ decreases the surface area being illuminated, reducing the emission current.

Figure 3(b) illustrates an almost linear behavior in the photoemission current from the CNT forest versus laser power. This suggests that emission is mainly through helping

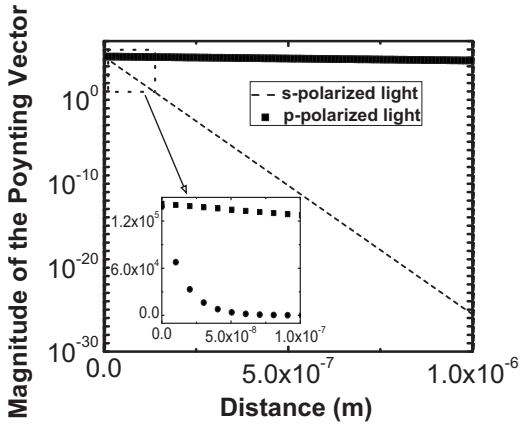

FIG. 4. The magnitude of the Poynting vector as it travels through a 1 μm thick CNT forest (logarithmic scale). Inset: nonlogarithmic plot of the first 100 nm. Notice the stronger absorption of s-polarized light.

electrons overcome the work function barrier, rather than nonlinear effects such as optical field-emission (where the tunneling barrier width is modulated by the light), which could happen at higher intensities.

In our experiments, approximately 20% of the laser beam covers the entire area of the side of the nanotube forest. Given the measured current of 40 nA, laser power of 100 mW, and photon energy of 4.66 eV, this indicates a quantum efficiency of $\sim 10^{-5}$, which is two orders of magnitude higher than the value reported for MWNT matts[8] and approaches the quantum efficiency of metallic photocathodes currently employed (i.e., Cu has a quantum efficiency in the order of $\sim 10^{-5}$ for 266 nm light[12]). We speculate that this value may be further improved by optimizing the structural parameters of the nanotube forest such as nanotube length and internanotube density. Photocathodes made from CNT forests would thus be promising for various applications, especially given that they are expected to be more robust and stable than conventional metallic surface photocathodes because of their complete and strong chemical structure.[13]

To further understand the photoemission behavior of CNT forests, we studied their optical properties using the effective optical constants of vertically aligned CNTs derived by García-Vidal *et al.*[14] and solving the electromagnetic wave equation based on a formalism we have developed previously.[15] Figure 4 illustrates the magnitude of the Poynting vector inside the nanotube forest for transverse-electric, 266 nm light incident at $\theta=90°$ on a 1 μm thick CNT forest. The simulations were done for two cases of polarization: electric field of the laser parallel (s-polarized) and perpendicular (p-polarized) to the axis of the nanotubes. It is evident that s-polarized light does not penetrate the CNT forest by much and, within the first 10 nm, the magnitude of the Poynting vector is reduced by an order of magnitude; almost all the light is absorbed within the first few tens of nanometers. On the other hand, p-polarized light is hardly absorbed even within the first micrometer. In our experiments, the UV laser was circularly polarized and we expect its absorption behavior to be somewhere between that of s- and p-polarized cases. Also, we recognize that these simulations only predict optical absorption and do not include the photoelectron emission process. Nonetheless, it is clear that most of the light does not penetrate deeper than a few tens of nanometers from the side of the forest, and whatever electron emission happens must happen from within that region potentially implying high emission current density. The calculated reflectance for these forests is $\sim 10^{-3}$, which is consistent with the observation of Yang *et al.*[16] and Mizuno *et al.*[17] who have reported that CNT forests are an extremely dark material.

As a side note, given the significant difference in the decay lengths of s- and p-polarized lights, a CNT forest could be used as an excellent polarizer, as previously demonstrated by Murakami *et al.*[18] These forests can also be shape engineered[19] to have sharp features to potentially improve their performance. They can also be grown on metallic contacts, which could then be easily integrated into accelerators and other electron-beam devices.

We demonstrated UV photoelectron emission from millimeter-long MWNT forests with quantum efficiencies in the order of $\sim 10^{-5}$ at low fields (pure photoemission) and $\sim 10^{-3}$ at an applied field of 0.3 V μm^{-1}. This is four orders of magnitude higher than the value reported for a matt of horizontal, randomly distributed MWNTs. Our simulations showed that the majority of the light is absorbed within the first few layers of the forest edge.

The authors acknowledge financial support from the Natural Sciences and Engineering Research Council (NSERC Grant Nos. 341629-07 and 361503-09), the Canada Foundation for Innovation (CFI), the British Columbia Knowledge Development Fund (BCKDF), BCFRST Foundation, and the British Columbia Innovation Council. P.Y. thanks the Department of Electrical and Computer Engineering and the University of British Columbia. M.M. thanks the Bullitt Foundation for a graduate fellowship.

[1]E. Lidorikis and A. C. Ferrari, ACS Nano **3**, 1238 (2009).
[2]K. G. Batrakov, S. A. Maksimenko, P. P. Kuzhir, and C. Thomsen, Phys. Rev. B **79**, 125408 (2009).
[3]P. G. O'Shea and H. P. Freund, Science **292**, 1853 (2001).
[4]C.-J. Chiang, K. X. Liu, and J. P. Heritage, Appl. Phys. Lett. **90**, 083506 (2007).
[5]D. Tasis, N. Tagmatarchis, A. Bianco, and M. Prato, Chem. Rev. (Washington, D.C.) **106**, 1105 (2006).
[6]N. H. Tran, M. A. Wilson, A. S. Milev, J. R. Bartlett, R. N. Lamb, D. Martin, and G. S. K. Kannangara, Adv. Colloid Interface Sci. **145**, 23 (2009).
[7]A. Nojeh, K. Ioakeimidi, S. Sheikhaei, and R. F. W. Pease, J. Appl. Phys. **104**, 054308 (2008).
[8]T.-H. Wong, M. C. Gupta, and C. Hernandez-Garcia, Nanotechnology **18**, 135705 (2007).
[9]W. B. Choi, D. S. Chung, J. H. Kang, H. Y. Kim, Y. W. Jin, I. T. Han, Y. H. Lee, J. E. Jung, N. S. Lee, G. S. Park, and J. M. Kim, Appl. Phys. Lett. **75**, 3129 (1999).
[10]L. Hudanski, E. Minoux, L. Gangloff, K. B. K. Teo, J. P. Schnell, S. Xavier, J. Robertson, W. I. Milne, D. Pribat, and P. Legagneux, Nanotechnology **19**, 105201 (2008).
[11]T. L. Westover, A. D. Franklin, B. A. Cola, T. S. Fisher, and R. Reifenberger, J. Vac. Sci. Technol. B **28**, 423 (2010).
[12]V. Nassisi, A. Beloglazov, E. Giannico, M. R. Perrone, and A. Rainò, J. Appl. Phys. **84**, 2268 (1998).
[13]G. D. A. Jorio and M. S. Dresselhaus, *Carbon Nanotubes*, Topics in Applied Physics, Vol. 111 (Springer, New York, 2008).
[14]F. J. García-Vidal, J. M. Pitarke, and J. B. Pendry, Phys. Rev. Lett. **78**, 4289 (1997).
[15]S. Khorasani, A. Nojeh, and B. Rashidian, Fiber Integr. Opt. **21**, 173 (2002).
[16]Z.-P. Yang, L. Ci, J. A. Bur, S.-Y. Lin, and P. M. Ajayan, Nano Lett. **8**, 446 (2008).
[17]K. Mizuno, J. Ishii, H. Kishida, Y. Hayamizu, S. Yasuda, D. N. Futaba, M. Yumura, and K. Hata, Proc. Natl. Acad. Sci. U.S.A. **106**, 6044 (2009).
[18]Y. Murakami, S. Chiashi, Y. Miyauchi, M. Hu, M. Ogura, T. Okubo, and S. Maruyama, Chem. Phys. Lett. **385**, 298 (2004).
[19]D. N. Futaba, K. Hata, T. Yamada, T. Hiraoka, Y. Hayamizu, Y. Kakudate, O. Tanaike, H. Hatori, M. Yumura, and S. Iijima, Nature Mater. **5**, 987 (2006).